



# Investigating the Mechanical and Durability Properties of Geopolymer Concrete Based on Granulated Blast Furnace Slag as Green Concrete

Mohammadhossein Mansourghanaei <sup>a\*</sup>

<sup>a</sup> Ph.D. in Civil Engineering, Department of Civil Engineering, Chalous Branch, Islamic Azad University, Chalous, Iran

**Journals-Researchers use only:** Received date: 2023.04.28; revised date: 2023.06.25; accepted date: 2023.07.06

## Abstract

Geopolymer concretes (GPCs) are known as green, environmentally friendly, sustainable concretes in the development of the structural industry with superior mechanical performance and durability compared to ordinary Portland cement concrete (OPCC). This type of concrete emits less CO<sub>2</sub> than OPCC and aims for efficient waste management while reducing environmental impacts. In this experimental research, 5 mixed designs were made of GPC based on granulated blast furnace slag (GBFS), which contains 0-8% Nano silica (NS) and 1-2% polyolefin fibers (POFs). A mixed design was also made of OPCC to compare with GPC. The tests of compressive strength, tensile strength, drop weight impact (DWI), Ultrasonic Pulse Velocity (UPV), water permeability and microstructural examination by scanning electron microscope (SEM) images and X-ray fluorescence (XRF) spectroscopy were performed on concrete samples and the results were analyzed and compared. The results obtained in this laboratory research, while overlapping with each other, indicate the superiority of mechanical properties and durability of GPC compared to OPCC. © 2017 Journals-Researchers. All rights reserved. (DOI: <https://doi.org/10.52547/JCER.5.3.24>)

**Keywords :** Geopolymer Concrete (GPC), Granulated Blast Furnace Slag (GBFS), Nano Silica (NS), Polyolefin Fibers (POFs), Mechanical and Durability Properties.

\* Corresponding Author. Tel: +989121712070; E-mail: Mhm.Ghanaei@iauc.ac.ir

## 1. Introduction

Cement is the second most consumed product (after water) in the world [1] and the third source of toxic carbon dioxide ( $\text{CO}_2$ ) emissions in the atmosphere [2] and it is estimated that cement is responsible for producing 5-8% of  $\text{CO}_2$  in the atmosphere. [2,3]. In this regard, with the production of one ton of cement, approximately one ton of  $\text{CO}_2$  gas is released into the atmosphere [4]. On the other hand, cement production requires high consumption of energy and mineral resources [5]. These challenges have led scientists to search for alternatives such as the production of green concrete or GPC [6]. GPC is emerging as one of the building materials [7]. GPC is produced from the process of geopolymerization, in which molecules known as oligomers are combined to form covalently bonded geopolymer networks [8]. The properties of GPC are determined based on the properties of the materials used and its processing conditions [9]. In this regard, the results showed that alkaline materials and active alkali solution (AAS) are the two main factors influencing the properties of GPC [10]. Environmentally friendly, stable and structurally sound GPC can be made from industrial waste (such as GBFS), municipal waste (such as construction waste) and agricultural waste (such as rice husk ash) [11,12]. The use of these wastes in the composition of GPC will lead to efficient waste management while reducing environmental pollution. Researchers' findings have shown that the use of industrial waste materials compared to ordinary cement in the composition of GPC also reduces the cost of concrete production [13]. It has been reported that the amount of  $\text{CO}_2$  produced in GPC is lower than ordinary Portland concrete (OPC) [7,14-18]. On the other hand, due to high compressive strength, low permeability and high resistance to acid attack, GPCs are a suitable alternative to OPCC in the construction of structures [8]. In the production of GPC, active alkali solutions such as potassium hydroxide (KOH), sodium hydroxide (NaOH), potassium silicate ( $\text{K}_2\text{SiO}_3$ ) or sodium silicate ( $\text{Na}_2\text{SiO}_3$ ) are needed for the geopolymerization of aluminosilicate precursors [19]. In this regard, the most commonly used combined active alkali solution in GPC is the use of sodium hydroxide (NaOH) and sodium silicate ( $\text{Na}_2\text{SiO}_3$ ), which have been used in several studies [20-22]. Hydrated gels are the main factor in creating bond and strength in the hardened GPC structure. In GPC based on GBFS, the production of hydrated gels

such as C-S-H, N-A-S-H and C-A-S-H is high in the geopolymerization process, and the largest volume of production belongs to C-S-H gel. Studies show that C-A-S-H gel is formed in the interfacial transition zones (ITZ) in the geopolymerization process of GPC based on GBFS, which helps to increase the compressive strength of this type of concrete compared to OPCC slow [23]. The amount of porosity and pores in the microstructure of GPC is less than that of OPCC, and this is one of the main factors of the superiority of mechanical properties and durability in GPC compared to OPCC. In this regard, the microscopic morphology of concrete samples with SEM images of the microstructure of GPC based on GBFS show more microstructure than OPCC (which has large pores) [6,23]. On the other hand, microstructure studies on GPC show better characteristics of ITZ compared to OPCC [24]. Also, studies have shown that increasing the curing temperature in GPC based on GBFS improves the laboratory results [25]. Industrial wastes such as GBFS, which often have unknown uses, are usually dumped in landfills, which lead to environmental pollution [26]. It has been estimated that for each ton of steel production, about 400 kg of steel furnace slag including GBFS and basic oxygen furnace slag (BOFS) are produced. GBFS contains siliceous (Si) and aluminate (Al) materials, the different amounts of which are used in the composition of concrete, can have a positive effect on the speed of the geopolymerization process [26]. On the other hand, GBFS helps in forming a larger volume of hydrated gels (compared to OPC) such as C-S-H in the composition of GPC [27]. Research has shown that the mechanical performance and durability of GPC based on GBFS is beyond that of OPCC [28-30]. The use of nanomaterials rich in aluminate and silicate particles in the composition of GBFS GPC leads to the improvement of mechanical properties in this type of concrete [12,31,32]. This issue is mostly due to the increase in the speed of the geopolymerization process and the greater participation of nanoparticles in the chemical reaction process in GPC [33]. In this regard, the addition of NS to the composition of GPC improves the mechanical properties of this type of concrete [34]. The use of fibers in the composition of concrete improves the mechanical properties and durability of concrete [35,36]. In this regard, the use of fibers improves the tensile strength of GPC [37], but the excessive use of fibers in the composition of

concrete causes a decrease in the mechanical properties of this type of concrete [38]. The type of fibers used clearly affects the compaction of concrete according to its density [39]. Research shows that the use of fibers in GPC improves the durability of concrete in the long term [40]. On the other hand, fibers improve tensile strength, increase energy absorption capacity, toughness and ductility in GPC [41]. In this laboratory study, increasing the mechanical properties and durability of GBFS NS and POFs is one of the innovative goals. On the other hand, according to the research of others, helping the healthy environment by reducing CO<sub>2</sub> emissions from conventional cement production, is another goal in this research.

## 2. Experimental Program


### 2.1 Materials

In this experimental study, the OPC type II with a 2.35 g/cm<sup>3</sup> of specific weight according to standard En 197-1 and the GBFS was used in powder form with the density of 2.75 g/cm<sup>3</sup> according to ASTM C989/C989M standard. The chemical properties of these materials are indicated in Table 1. The NS particles made up of 99.5% SiO<sub>2</sub> with an average diameter in the range of 15 to 25 nm were used. Crimped POFs according to ASTM D7508/D7508M standard, 30 mm in length, were also used, whose physical properties are shown in Fig. 1. The used fine aggregates were natural clean sand with a fineness modulus of 2.95 and a density of 2.75 g/cm<sup>3</sup>, and the coarse aggregates were crushed gravel with a maximum size of 19 mm and a density of 2.65 g/cm<sup>3</sup> according to the requirements of the ASTM-C33. In this research, thermal curing of GPC has been done at 60 °C for 48 hours in an electric furnace under 80±3% relative humidity. In this regard, research has shown that thermal curing of GPC based on GBFS leads to improvement of mechanical properties and durability in concrete [28,16].

### 2.2 Mix Design

For accurate investigation, six mixture designs were considered, according to ACI 211.1-89 standard. For GPC, as in other articles [28,42], a OPCC mixing scheme was used. The first sample included a regular concrete containing Portland cement where the water to cement ratio has considered to be constantly 0.45. Five other samples include GPC with different NS

and POFs. The GPC samples are generally categorized into two groups: the first group lacks POFs with the NS amount of 0-8%. The second group contains 8% of NS, where the POFs are used in these designs in the form of 1 and 2 percent. In order to achieve the same performance in each mixture design and obtain a slump of about 20 ±100 mm, we have used normal polycarboxylate based superplasticizers. Besides, 202.5 kg/m<sup>3</sup> of the alkaline solution is used in this case. The used alkaline solution is a combination of NaOH and Na<sub>2</sub>SiO<sub>3</sub> with the weight ratio of 2.5, utilized with the mixture specific weight of 1483 kg/m<sup>3</sup> and the concentration of 12 M. The conducted studies indicate that due to the significant level of C-S-H formation when utilizing Na<sub>2</sub>SiO<sub>3</sub>, using a combination of NaOH and Na<sub>2</sub>SiO<sub>3</sub> increases the compressive strength compared to single employment of CaOH [43]. The samples mixture design is indicated in Table 2.



Tensile Strength (N/mm <sup>2</sup> )	>500
Length (mm)	30
Diameter (mm)	0.8
Elasticity Modulus (GPa)	>11
Bulk Density (g/cm <sup>3</sup> )	0.910

Fig. 1. Physical Properties of the POFs

Table 1

Chemical Compositions of Materials (%)

Component	GBFS	OPC
SiO <sub>2</sub>	29.2	21.3
Al <sub>2</sub> O <sub>3</sub>	19.4	4.7
Fe <sub>2</sub> O <sub>3</sub>	5.8	4.3
CaO	38.6	62.7
MgO	2.8	2.1
SO <sub>3</sub>	2.6	2
K <sub>2</sub> O	0.1	0.65
Na <sub>2</sub> O	0.2	0.18
TiO <sub>2</sub>	0.6	-
Free Cao	-	1.12
LOI	0.3	1.84

Table 2  
Details of the Mix Designs

Mix ID	OPC	GBFS	Water	AAS	NS	Coarse Aggregates (Kg/m <sup>3</sup> )	Fine Aggregates	POFs	Super Plasticizer	
1	OPCC	450	0	202.5	0	0	1000	761	0	6.75
2	GPCNS0POF0	0	450	0	202.5	0	1000	816	0	6.75
3	GPCNS4POF0	0	432	0	202.5	18	1000	767	0	7.8
4	GPCNS8POF0	0	414	0	202.5	36	1000	718	0	8.3
5	GPCNS8POF1	0	432	0	202.5	36	1000	672	24	8.6
6	GPCNS8POF2	0	432	0	202.5	36	1000	646	48	9

### 2.3 Test Methods

After fabricating the samples, for better curing and increasing the resistance properties, the samples were placed in an oven at 60 °C with a thermal rate of 4.4 °C/min for 48 h. In this study, the compressive strength tests were performed on 10-cm<sup>3</sup> cubic specimens based on BS EN 12390. to determine the tensile strength of the cylindrical specimens (15 cm in diameter and 30 cm in length), the splitting tests were conducted based on ASTM C496. The concrete's resistance to dynamic loads (impacts) was measured using the drop weight hammer test according to the report by the ACI 544-2R committee. This test was conducted with repeating impacts on disks with a diameter of 15 cm and a height of 63.5 cm. The UPV tests were conducted according to ASTM C597 using a non-destructive ultrasonic electronic apparatus, PUNDIT MODEL PC1012, with an accuracy of  $\pm 0.1 \mu s$  for a transformer with a vibrational frequency of 55 kHz and a movement time accuracy of  $\pm 2\%$  for the distance. According to EN 12390-8, the water permeability tests were performed on 150×150×150-mm<sup>3</sup> cubic specimens with a water pressure of 50±500 kPa on a circular area with a diameter of 75 mm on one of the surfaces for 72 hours. In this article, the tests of compressive strength, tensile strength, DWI, UPV, water permeability in concrete at the curing age of 7, 28 and 90 days were performed. XRF analysis at 7 days curing age and SEM analysis at 90 days curing age were performed on concrete samples.

## 3. Results and Discussion

### 3.1 Results of the Compressive Strength Test

The results of the compressive strength test of concrete samples in this laboratory research are shown in Figure 2. Figure 3 shows the concrete samples in each mix design after performing the compressive strength test at the age of 90 days curing. Based on the results, it can be seen that increasing the curing age in the concrete of each design has led to an improvement in compressive strength. This issue is due to the progress of the chemical reaction process and the production of a higher volume of hydrated gels such as C-S-H in the concrete composition at the same time as the age curing of the concrete increases [44].

By increasing NS particles in GPC, the compressive strength of concrete has improved. This is due to the increase in the rate of polymerization and the production of more volume of hydrated gels in the composition of GPC [33]. The increase of POFs in the composition of GBFS-based GPC has led to a drop in the compressive strength results of this type of concrete. This issue can be due to the type of fibers used and the improper bonding of fibers with geopolymeric mortar in the interfacial transition zone (ITZ). Design GPCNS8POF0 is the best plan in terms of achieving compressive strength, so that at the age of 90 days curing, it has achieved a 33% better result than design OPCC and 29% better than design GPCNS0POF2.

### 3.2 Results of the Tensile Strength Test

Figure 4 shows the results of the tensile strength test in this laboratory research. Figure 5 includes the concrete samples of all the mixed designs after the tensile strength test. Based on the results, increasing the age of concrete curing has led to improved results in all designs. In this regard, OPCC with 93% increase in GPC design GPCNS4POF0 with 72% increase was a step forward. In GPCs, the addition of NS has led to the improvement of tensile strength results in concrete, in this regard, at the age of 90 days of curing (as the best curing age), design GPCNS8POF0 with 8% NS obtained 15% higher tensile strength than design GPCNS0POF0 without NS. The addition of up to 2% POFs in the GPC mixture led to the improvement of the tensile strength test results in this research. So that at the age of 90 days, design GPCNS8POF2 (containing 2% POFs) obtained 8% more tensile strength than design GPCNS8POF0 (without POFs). This issue is mostly due to the proper bonding of POFs in the GPC composition under Brazilian tensile test loading [45,46]. The findings of scientists have shown that the use of different types of fibers such as natural kenaf [47] and glass fibers [48] in the composition of GPC leads to the improvement of tensile strength in this type of concrete.

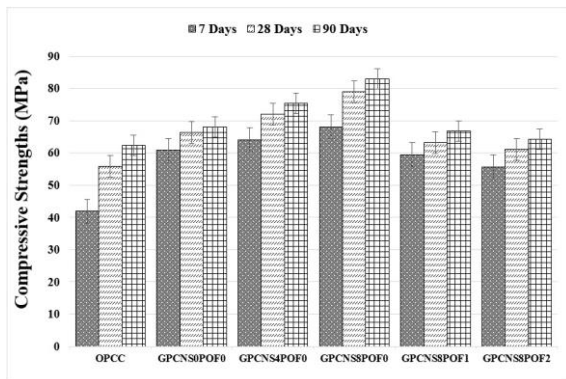


Fig. 2. The Compressive Strengths of the Specimens



Fig. 3. Concrete Sample in Compressive Strength Test

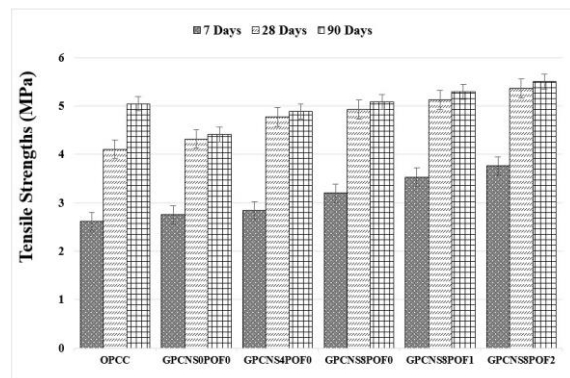


Fig. 4. The Tensile Strengths of the Specimens



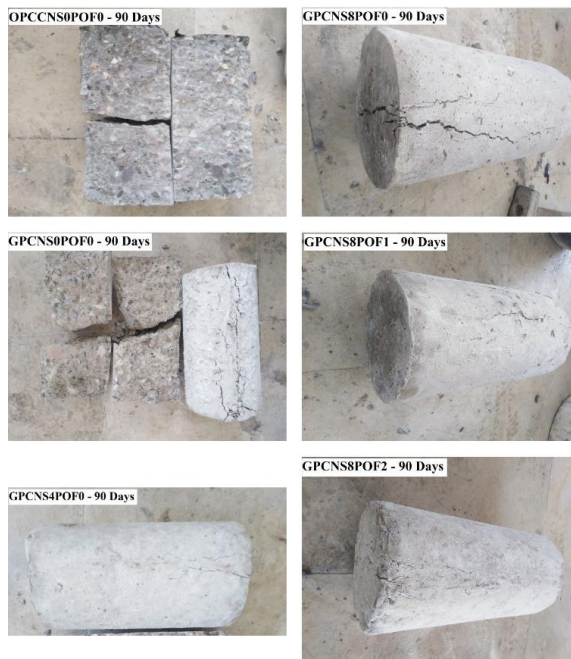


Fig. 5. Concrete Sample in Tensile Strength Test

### 3.3 Results of the DWI Test

The results of the impact test using the drop weight method under the initial impact energy for the occurrence of the initial crack ( $E_1$ ), the impact energy of the final crack ( $E_2$ ) and the flexibility index ( $E_2/E_1$ ) of the concrete samples of all designs at the age of 90 days and at the ambient temperature (21-25 °C) based on Joule is shown in the diagram of Figure 6. Figure 7 shows the device for performing the DWI test. According to the results, it can be seen that the impact energy of breaking ( $E_2$ ) the concrete sample in all designs is more than the impact energy for the initial crack ( $E_1$ ). The initial and final energy values for cracking and failure of the OPCC sample were lower than the corresponding values in all GPC designs. The addition of POFs up to 2% to the GPC composition led to the improvement of the resistance of concrete samples against the DWI. So that in design GPCNS8POF2, the amount of initial energy ( $E_1$ ) increased by 30% and final energy ( $E_2$ ) by 3.4 times compared to design GPCNS8POF0. In this regard, the amount of initial energy in design GPCNS8POF2 concrete was increased by 2.3 times and the final energy was increased by 7 times compared to OPCC. Flexibility index ( $E_2/E_1$ ) in GPC samples improved by increasing the amounts of NS

and POFs. The findings of other researchers show that GBFS based GPCs have better impact resistance than OPCCs [49]. Also, in GPCs, the addition of fibers leads to the improvement of concrete resistance against impact loads [30]. The use of other types of fibers, such as in the composition of GPC, increases the resistance of this type of concrete against impact loads [50].

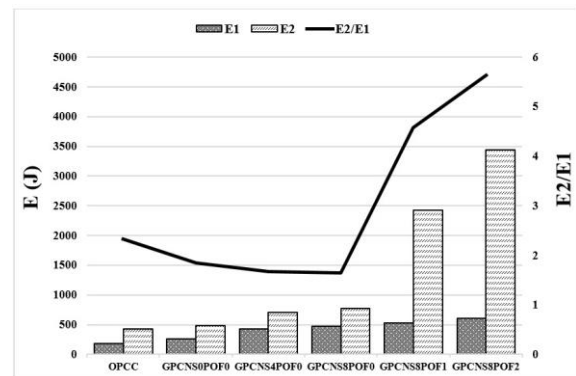


Fig. 6. The Impact of the Specimens



Fig. 7. DWI Test Machine

### 3.4 Results of The UPV Test

Figure 8 shows the results of UPV test on concrete samples in this research. Increasing the curing age in concrete due to the progress of the hydration and geopolymerization process in concrete has led to the improvement of UPV [28]. The addition of NS to the GPC composition leads to the production of more hydrated gels in concrete, and thus the amount of UPV has increased. The addition of polyolefin fibers to the GPC composition has led to a decrease in UPV results. In this regard, at the processing age of 90 days (as the best curing age), adding POFs to design 6 has led to a reduction of 12% in the results compared to design 4 (without POFs). UPV in OPCC at all ages is higher than UPV in GPC at corresponding ages. This issue is due to the appearance of microcracks during the thermal curing process in GPC, which has been effective on the UPV loss. In the diagram of Figure 8, the quality of concrete is determined based on the speed of waves passing through concrete according to the IS 13311-1 standard. In this regard, it can be seen that at the age of 7 days curing, concrete designs GPCNS0POF0 and GPCNS8POF0 have excellent quality and other designs are in good quality. At the age curing of 28 and 90 days, all concrete designs are of excellent quality.

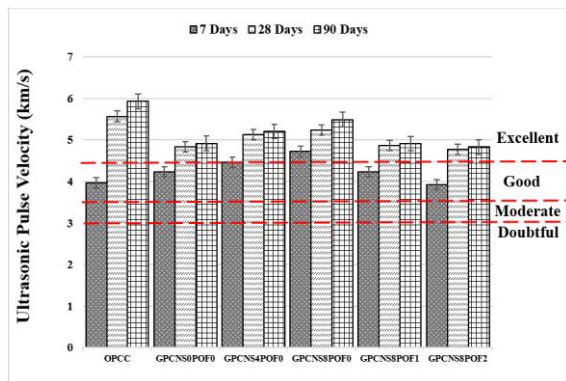


Fig. 8. The UPV of The Specimens

### 3.5 Results of the Water Permeability Test

The results of the water permeability test in concrete based on the depth of water penetration (in mm) in concrete are shown in the diagram of Figure 9. Based on these results, it can be seen that in each design, the depth of water penetration in concrete decreases with

the increase of curing age in concrete. This issue has become harder due to the improvement of concrete density and the increase of adhesion between concrete components, which is completed by the development of the chemical process. The depth of water penetration in GPC is less than OPCC at the corresponding age, this shows the superior performance of durability in GPC compared to OPCC. The addition of NS in the composition of GPC with the improvement of the matrix of the geopolymeric structure led to a decrease in water permeability by 35% (design GPCNS8POF0 compared to design GPCNS0POF0 in 28 days of curing) in this type of concrete. The addition of POFs up to 2% in the composition of GPC led to a decrease in the depth of water penetration in this type of concrete up to 27% (design GPCNS8POF2 compared to design GPCNS8POF0). Figure 10 shows concrete samples undergoing water permeability test.

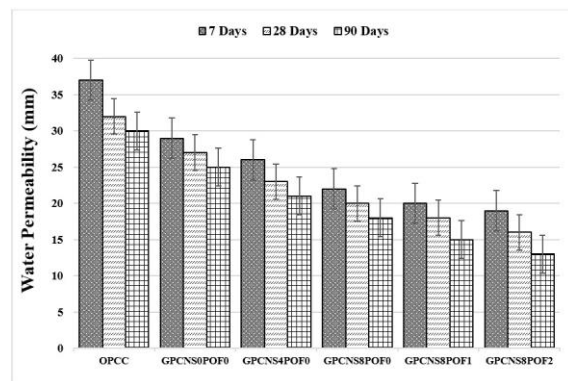


Fig. 9. The Water Permeability of The Specimens



Fig. 10. Water Permeability Test in Concrete

### 3.6 Results of The XRF Analysis

The results of XRF analysis of concrete samples are shown in Table 3.  $\text{SiO}_2$ ,  $\text{Al}_2\text{O}_3$  and  $\text{CaO}$  are seen as the three main elements with the highest amount in all designs. In this regard,  $\text{SiO}_2$  amounts in plans 4, 5 and 6 (including GPC containing 8% NS) have reached the highest value (about 37%). The lowest amount of  $\text{SiO}_2$  (27%) is found in OPCC.  $\text{Al}_2\text{O}_3$  is found in the range of 7-8% in GPC designs, and it has reached the lowest amount (5.6%) in OPCC designs. The maximum (37%) of  $\text{CaO}$  is seen in OPCC and the maximum (26.8%) and minimum (15.3%) of  $\text{CaO}$  is seen in concrete design 2 and 5 of GPC, respectively. LOI values in all designs are in the same range (about 16%).  $\text{SiO}_2$  and  $\text{Al}_2\text{O}_3$  are the main elements in slag and NS (primary materials of GPC), on the other hand,  $\text{CaO}$  is also the main element of OPC in OPCC.

Table 3  
XRF Test Results (%)

Component	Mix NO					
	1	2	3	4	5	6
$\text{SiO}_2$	27.1	19.5	32.02	36.3	37	36/8
$\text{Al}_2\text{O}_3$	5.6	8	6.7	7.01	7/1	6/9
$\text{CaO}$	37.1	26.8	23.6	15.2	15/13	15/18
$\text{Na}_2\text{O}$	1.1	15.1	9.01	12.8	12/64	13/01
$\text{Fe}_2\text{O}_3$	7.2	5.6	3.9	3.94	3/79	4
$\text{MgO}$	2.1	5.05	4.01	3.01	3/15	2/89
$\text{K}_2\text{O}$	0.9	1.01	1.01	1.05	1/12	1/14
$\text{SO}_3$	1.6	1.1	1.87	2.8	1/9	1/98
$\text{TiO}_2$	0.4	0.9	1.08	1.1	1	1/2
$\text{P}_2\text{O}_5$	0.1	0.1	0.14	0.1	0/139	0/153
$\text{MnO}$	0.1	0.4	0.65	0.6	0/64	0/71
LOI	16.4	16.04	15.9	15.7	16	15/9

### 3.7 Results of the SEM Analysis

The results of SEM analysis are shown in Figure 11. In the composition of ordinary concrete compared to GPC, the amount of hydrated gels (C-S-H) is seen in its lowest amount. Also, the tree structure (which shows the low density of concrete), unhydrated particles and pores in the composition of OPCC is more than the design of GPC. In GPC designs, the amount of hydrated gels has been increased by increasing the amount of NS in the designs. This process is due to the acceleration of geopolymerization activity and the production of a

larger volume of hydrated gels in this type of concrete. The researchers' findings show that GPCs have superior microstructural characteristics than OPCCs [51,52]. Adding materials containing aluminosilicate sources to the composition of GPC adds its characteristics [24]. This superiority is often due to the presence of dispersed pores with very small sizes in the matrix of GPC compared to OPCC [6].

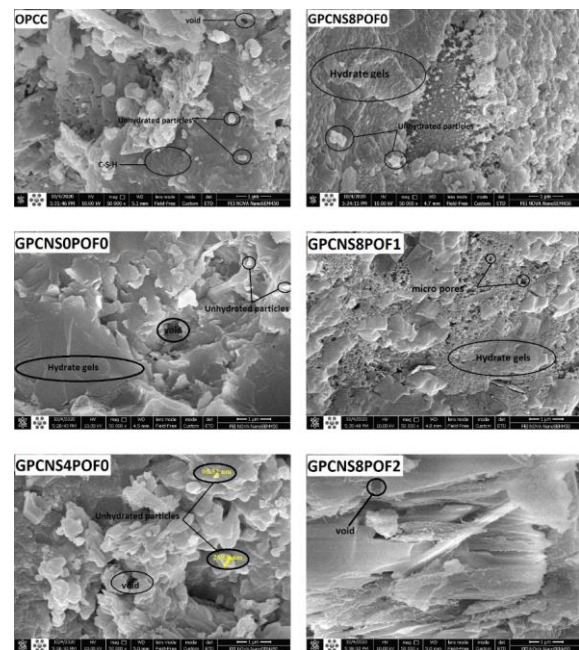


Fig. 11. SEM Image

## 4. Conclusions

In this article, tests of compressive strength, tensile strength, DWI, UPV, water permeability in OPCC and GPC at the curing age of 7, 28 and 90 days were performed and the results were compared and analyzed. XRF analysis at the curing age of 7 days and SEM analysis at the curing age of 90 days were performed on concrete samples and the results were evaluated. The most important results in this research are as follows.

1. Except for the UPV test, the results in all tests show the superiority of GPC over OPCC. This shows the superior performance of GBFS-based GPC compared to OPCC.



2. Due to the thermal curing in GPC that has led to microcracks, the UPV results in this type of concrete are lower than OPCC.
3. In GPC, the addition of NS has improved the results in all tests. This issue is due to the help of NS to accelerate the geopolymerization process and produce more volume of hydrated gels in the GPC matrix.
4. In GPC, the addition of POFs has improved the results in tensile strength, DWI and water permeability tests. In this regard, the addition of fibers has been appropriate to prevent crack propagation and maintain the localization of cracks.
5. The type of fiber and its connection method in GBFS-based GPC has led to a drop in results in compressive strength and UPV tests.
6. The results of XRF and SEM analysis are in agreement and overlapping with other results in this laboratory research.

## References

- [1] Alanqari, K., Al-Yami, A., & Wagle, V. (2022, February). Preparation of a Synthetic Geopolymer Cement Utilizing Saudi Arabian Volcanic Ash for a Sustainable Development: Method, Preparation and Applications. In International Petroleum Technology Conference.
- [2] Vijayashankar, T., Girinath, T., Dineshkumar, S., & Saravanaganesh, S. (2022). EXPERIMENTAL STUDY ON GEOPOLYMER CONCRETE USING HEAVY WEIGHT AGGREGATE. 04 (06).
- [3] Li, L., Wei, Y. J., Li, Z., & Farooqi, M. U. (2022). Rheological and viscoelastic characterizations of fly ash/slag/silica fume-based geopolymer. *Journal of Cleaner Production*, 354, 131629.
- [4] Nishanth, L., Patil, N. N., Kumbar, N., Kaveti, S., & Kar, D. (2022). Influence of E-Coli on workability and strength characteristics of self-consolidating geopolymer concrete based on GGBFS, flyash and alccofine. *Materials Today: Proceedings*.
- [5] Yang, S., Zhao, R., Ma, B., Si, R., & Zeng, X. (2023). Mechanical and fracture properties of fly ash-based geopolymer concrete with different fibers. *Journal of Building Engineering*, 63, 105281.
- [6] Amin, M., Elsakhawy, Y., Abu el-hassan, K., & Abdelsalam, B. A. (2022). Behavior evaluation of sustainable high strength geopolymer concrete based on fly ash, metakaolin, and slag. *Case Studies in Construction Materials*, 16, e00976.
- [7] Amran, M., Huang, S. S., Debbarma, S., & Rashid, R. S. (2022). Fire resistance of geopolymer concrete: A critical review. *Construction and Building Materials*, 324, 126722.
- [8] Wong, L. S. (2022). Durability performance of geopolymer concrete: A review. *Polymers*, 14(5), 868.
- [9] Saif, M. S., El-Hariri, M. O., Sarie-Eldin, A. I., Tayeh, B. A., & Farag, M. F. (2022). Impact of Ca<sup>+</sup> content and curing condition on durability performance of metakaolin-based geopolymer mortars. *Case Studies in Construction Materials*, 16, e00922.
- [10] Feng, B., & Liu, J. (2022). Durability of Repair Metakaolin Geopolymeric Cement under Different Factors. *Processes*, 10(9), 1818.
- [11] Shehata, N., Mohamed, O. A., Sayed, E. T., Abdelkareem, M. A., & Olabi, A. G. (2022). Geopolymer concrete as green building materials: Recent applications, sustainable development and circular economy potentials. *Science of the Total Environment*, 155577.
- [12] Shilar, F. A., Ganachari, S. V., Patil, V. B., Nisar, K. S., Abdel-Aty, A. H., & Yahia, I. S. (2022). Evaluation of the Effect of Granite Waste Powder by Varying the Molarity of Activator on the Mechanical Properties of Ground Granulated Blast-Furnace Sla.
- [13] Das, S., Saha, P., Jena, S. P., & Panda, P. (2022). Geopolymer concrete: Sustainable green concrete for reduced greenhouse gas emission—A review. *Materials Today: Proceedings*, 60, 62-71.
- [14] Rajmohan, B., Nayaka, R. R., Kumar, K. R., & Kaleemuddin, K. (2022). Mechanical and durability performance evaluation of heat cured low calcium fly ash based sustainable geopolymer concrete. *Materials Today: Proceedings*, 58, 1337-1343.
- [15] Chavda, D. C., Pitroda, J. R., & Vaghela, K. Experimental Study on Geopolymer Concrete Using Waste Ceramic Powder: A Review.
- [16] Öz, A., Bayrak, B., Kavaz, E., Kaplan, G., Çelebi, O., Alcan, H. G., & Aydın, A. C. (2022). The radiation shielding and microstructure properties of quartzic and metakaolin based geopolymer concrete. *Construction and Building Materials*, 342, 127923.
- [17] El-Mir, A., El-Hassan, H., El-Dieb, A., & Alsallamin, A. (2022). Development and Optimization of

- Geopolymers Made with Desert Dune Sand and Blast Furnace Slag. *Sustainability*, 14(13), 7845.
- [18] Yoo, D. Y., Lee, S. K., You, I., Oh, T., Lee, Y., & Zi, G. (2022). Development of strain-hardening geopolymer mortar based on liquid-crystal display (LCD) glass and blast furnace slag. *Construction and Building Materials*, 331, 127334.
- [19] Kheimi, M., Aziz, I. H., Abdullah, M. M. A. B., Almadani, M., & Abd Razak, R. (2022). Waste Material via Geopolymerization for Heavy-Duty Application: A Review. *Materials*, 15(9), 3205.
- [20] Zeyad, A. M., Magbool, H. M., Tayeh, B. A., de Azevedo, A. R. G., Abutaleb, A., & Hussain, Q. (2022). Production of geopolymer concrete by utilizing volcanic pumice dust. *Case Studies in Construction Materials*, 16, e00802.
- [21] Bhaskar, M. U., & Prashanth, M. (2022). SILICAFUME BASED GEOPOLYMER CONCRETE-DURABILITY PROPERTIES FOR M60 GRADE. *NeuroQuantology*, 20(6), 5415-5425.
- [22] Arunachalam, N., Maheswaran, J., Chellapandian, M., Murali, G., & Vatin, N. I. (2022). Development of High-Strength Geopolymer Concrete Incorporating High-Volume Copper Slag and Micro Silica. *Sustainability*, 14(13), 7601.
- [23] Bellum, R. R., Al Khazaleh, M., Pilla, R. K., Choudhary, S., & Venkatesh, C. (2022). Effect of slag on strength, durability and microstructural characteristics of fly ash-based geopolymer concrete. *Journal of Building Pathology and Rehabilitation*, 7(1), 1.
- [24] Thomas, B. S., Yang, J., Bahurudeen, A., Chinnu, S. N., Abdalla, J. A., Hawileh, R. A., ... & Hamada, H. M. (2022). Geopolymer concrete incorporating recycled aggregates: A comprehensive review. *Cleaner Materials*, 100056.
- [25] Farokhzad, R., Mohammadbeigi, A. (2022). Evaluating Compressive and Tensile Strength and Water Absorption of Geopolymer Mortar Containing Slag (GGBFS) in Comparison with Pozzolan Metakaolin. *Journal of Structural and Construction Engineering*, 8(11), 292-3.
- [26] Shilar, F. A., Ganachari, S. V., Patil, V. B., Khan, T. Y., Almakayeel, N. M., & Alghamdi, S. (2022). Review on the relationship between nano modifications of geopolymer concrete and their structural characteristics. *Polymers*, 14(7), 1421.
- [27] Li, B., Tang, Z., Huo, B., Liu, Z., Cheng, Y., Ding, B., & Zhang, P. (2022). The Early Age Hydration Products and Mechanical Properties of Cement Paste Containing GBFS under Steam Curing Condition. *Buildings*, 12(10), 1746.
- [28] Mansourghanaei, M., Biklaryan, M., & Mardookhpour, A. (2022). Experimental study of the effects of adding silica nanoparticles on the durability of geopolymer concrete. *Australian Journal of Civil Engineering*, 1-13.
- [29] Mansourghanaei, M., Biklaryan, M., & Mardookhpour, A. (2022). Experimental study of properties of green concrete based on geopolymer materials under high temperature. *Civil Engineering Infrastructures Journal*.
- [30] Mansourghanaei, M. (2022). Experimental evaluation of compressive, tensile strength and impact test in blast furnace slag based geopolymer concrete, under high temperature. *Journal of Civil Engineering Researchers*, 4(2), 12-21.
- [31] Mansourghanaei, M., Biklaryan, M., & Mardookhpour, A. (2023). Experimental Study of Modulus of Elasticity, Capillary absorption of water and UPV in Nature-Friendly Concrete Based on Geopolymer Materials. *International Journal of Advanced Structural Engine*.
- [32] Xavier, C. S. B., & Rahim, A. (2022). Nano aluminium oxide geopolymer concrete: An experimental study. *Materials Today: Proceedings*, 56, 1643-1647.
- [33] Han, Q., Zhang, P., Wu, J., Jing, Y., Zhang, D., & Zhang, T. (2022). Comprehensive review of the properties of fly ash-based geopolymer with additive of nano-SiO<sub>2</sub>. *Nanotechnology Reviews*, 11(1), 1478-1498.
- [34] Jin, Q., Zhang, P., Wu, J., & Sha, D. (2022). Mechanical Properties of Nano-SiO<sub>2</sub> Reinforced Geopolymer Concrete under the Coupling Effect of a Wet-Thermal and Chloride Salt Environment. *Polymers*, 14(11), 2298.
- [35] Li, L., Sun, H. X., Zhang, Y., & Yu, B. (2021). Surface cracking and fractal characteristics of bending fractured polypropylene fiber-reinforced geopolymer mortar. *Fractal and Fractional*, 5(4), 142.
- [36] Li, L., Tao, J. C., Zhang, Y., Sun, H. X., Yuen, K. V., & You, P. B. (2022). Crack fractal analysis of fractured polyethylene fiber reinforced alkali activated mortar under flexural load. *Construction and Building Materials*, 345, 128428.

- [37] Lao, J. C., Xu, L. Y., Huang, B. T., Dai, J. G., & Shah, S. P. (2022). Strain-hardening ultra-high-performance geopolymer concrete (UHPGC): Matrix design and effect of steel fibers. *Composites Communications*, 30, 101081.
- [38] Xu, Z., Wu, J., Zhao, M., Bai, Z., Wang, K., Miao, J., & Tan, Z. (2022). Mechanical and microscopic properties of fiber-reinforced coal gangue-based geopolymer concrete. *Nanotechnology Reviews*, 11(1), 526-543.
- [39] Zeyad, A. M., Hakeem, I. Y., Amin, M., Tayeh, B. A., & Agwa, I. S. (2022). Effect of aggregate and fibre types on ultra-high-performance concrete designed for radiation shielding. *Journal of Building Engineering*, 58, 104960.
- [40] Li, W., Shumuye, E. D., Shiyang, T., Wang, Z., & Zerfu, K. (2022). Eco-friendly fibre reinforced geopolymer concrete: A critical review on the microstructure and long-term durability properties. *Case Studies in Construction Materials*, e00894.
- [41] Laxmi, G., & Patil, S. G. (2022). Effect of fiber types, shape, aspect ratio and volume fraction on properties of geopolymer concrete—A review. *Materials Today: Proceedings*.
- [42] Chokkalingam, P., El-Hassan, H., El-Dieb, A., & El-Mir, A. (2022). Development and characterization of ceramic waste powder-slag blended geopolymer concrete designed using Taguchi method. *Construction and Building Materials*, 349, 128744.
- [43] Pilehvar, S., Cao, V. D., Szczotok, A. M., Carmona, M., Valentini, L., Lanzón, M., ... & Kjøniksen, A. L. (2018). Physical and mechanical properties of fly ash and slag geopolymer concrete containing different types of micro-encapsulated phase change materials. *Construction and Building Materials*, 173, 28-39.
- [44] Zhang, F., Li, Y., Zhang, J., Gui, X., Zhu, X., & Zhao, C. (2022). Effects of slag-based cementitious material on the mechanical behavior and heavy metal immobilization of mine tailings based cemented paste backfill. *Heliyon*, e10695.
- [45] Wang, Y., Zhong, H., & Zhang, M. (2022). Experimental study on static and dynamic properties of fly ash-slag based strain hardening geopolymer composites. *Cement and Concrete Composites*, 129, 104481.
- [46] Aisheh, Y. I. A., Atrushi, D. S., Akeed, M. H., Qaidi, S., & Tayeh, B. A. (2022). Influence of polypropylene and steel fibers on the mechanical properties of ultra-high-performance fiber-reinforced geopolymer concrete. *Case Studies in Construction Materials*.
- [47] Abbas, A. G. N., Aziz, F. N. A. A., Abdan, K., Nasir, N. A. M., & Huseien, G. F. (2023). Experimental evaluation and statistical modeling of kenaf fiber-reinforced geopolymer concrete. *Construction and Building Materials*, 367, 130228.
- [48] Ali, S., Sheikh, M. N., & Hadi, M. N. (2023). Splitting-and Direct-Tensile Strengths of Ambient Cured Geopolymer Concrete with Glass Fibers. In *8th International Conference on Advanced Composite Materials in Bridges and Structures* (pp. 109-117). Springer, Cham.
- [49] Xie, J., Zhao, J., Wang, J., Fang, C., Yuan, B., & Wu, Y. (2022). Impact behaviour of fly ash and slag-based geopolymeric concrete: The effects of recycled aggregate content, water-binder ratio and curing age. *Construction and Building Materials*, 331, 127.
- [50] Wang, Z., Bai, E., Huang, H., Liu, C., & Wang, T. (2023). Dynamic mechanical properties of carbon fiber reinforced geopolymer concrete at different ages. *Ceramics International*, 49(1), 834-846.
- [51] Ahmed, M. F., Khalil, W. I., & Frayyeh, Q. J. (2022). Effect of Waste Clay Brick on the Modulus of Elasticity, Drying Shrinkage and Microstructure of Metakaolin-Based Geopolymer Concrete. *Arabian Journal for Science and Engineering*, 1-13.
- [52] Kaya, M., Koksall, F., Gencel, O., Munir, M. J., & Kazmi, S. M. S. (2022). Influence of micro Fe<sub>2</sub>O<sub>3</sub> and MgO on the physical and mechanical properties of the zeolite and kaolin based geopolymer mortar. *Journal of Building Engineering*, 52, 104443.